Physics Procedia

Volume 75, 2015, Pages 1381–1388

20th International Conference on Magnetism

Predictions of a Large Magnetocaloric Effect in Co- and Cr-Substituted Heusler Alloys Using First-Principles and Monte Carlo Approaches

Vladimir V. Sokolovskiy[1], Vasiliy D. Buchelnikov[1], Mikhail A. Zagrebin[1], Anna Grünebohm[2], and Peter Entel[2]

[1] Chelyabinsk State University, Chelyabinsk, Russia
vsokolovsky84@mail.ru, buche@csu.ru, miczag@mail.ru,
[2] University of Duisburg-Essen, Duisburg, Germany
anna@thp.uni-due.de, entel@thp.uni-due.de

Abstract

The effect of Co- and Cr-doping on magnetic and magnetocaloric poperties of Ni-Mn-(In, Ga, Sn, and Al) Heusler alloys has been theoretically studied by combining first principles with Monte Carlo approaches. The magnetic and magnetocaloric properties are obtained as a function of temperature and magnetic field using a mixed type of Potts and Blume-Emery-Griffiths model where the model parameters are obtained from *ab initio* calculations. The Monte Carlo calculations allowed to make predictions of a giant inverse magnetocaloric effect in partially new hypothetical magnetic Heusler alloys across the martensitic transformation.

Keywords: Heusler alloys, magnetocaloric effect, *ab initio* and Monte Carlo methods

1 Introduction

Nowadays, the search for new magnetocaloric materials with better magnetocaloric effect (MCE) as refrigerants is an important objective for the development of this technology [9, 8, 12, 2, 7, 13]. The MCE strongly depends on the type of magnetic phase transition. It is large in case of a first-order transition which involves significant latent heat and hysteresis. For many alloys (Gd-Ge-Si, Mn-As-Fe-P, Ni-Mn-Ga etc.)[9] with the ferro-to-paramagnetic (FM-PM) phase transition, the MCE is direct (conventional), i.e., the entropy change (ΔS_{mag}) decreases upon an isothermally applied magnetic field ($\Delta S_{mag} < 0$), and materials heat up when the field is adiabatically applied ($\Delta T_{ad} > 0$). On the other hand, for samples with antiferro-to-ferromagnetic (AFM-FM) phase transition (Fe-Rh[7], La-Fe-Al[9], $Mn_{2-x}Cr_xSb$[9], Mn_3GaC[9, 3], Ni-Mn-(In, Sn, Sb)[12, 2] etc.) the opposite behavior is observed. Namely, the samples are found to cool down under adiabatic condition if a magnetic field is applied

Selection and peer-review under responsibility of the Scientific Programme Committee of ICM 2015

doi:10.1016/j.phpro.2015.12.155

($\Delta T_{ad} < 0$) and entropy increases when the field is isothermally applied ($\Delta S_{mag} > 0$). Such behavior characterizes the inverse MCE.

Among magnetocaloric materials, Ni-(Co)-Mn-Z (Z = Ga, In, Sn, Sb) Heusler alloys can exhibit both the conventional and inverse MCE in dependence on composition and chemical disorder [12, 2, 10, 4, 6]. The inverse MCE arises from the AFM coupling between nearest Mn_Y-Mn_Z atoms. Here, Mn_Y and Mn_Z refer to Mn located on the original Mn sites and on the Z sites, respectively. Moreover, the AFM interaction in martensite is several times stronger than in austenite. As a result, a large difference in magnetization appears and yields the magnetization drop at a martensitic transition temperature T_m. According to different contributions of magnetic and structural entropies in austenite and martensite, the inverse MCE is achieved across T_m while the direct MCE appears near the Curie temperature (T_C) of austenite. We would like to point out that kind of breakthrough regarding of Co-doped Ni-Mn-In alloys has recently been achieved by Liu *et al.*[10] observing the giant inverse MCE ($\Delta T_{ad} \approx -6.2$ K at 317 K) and direct MCE ($\Delta T_{ad} \approx 2$ K at 400 K) in $Ni_{45}Co_5Mn_{37}In_{13}$ under the magnetic field change of 1.9 T. At present, this value of ΔT_{ad} is the record value among all Heusler alloys.

This paper addresses the question of a rise in the inverse MCE in Ni-Mn-(In, Sn, Ga, and Al) Heusler alloys by way of the substitution of Co and Cr atoms. Our hypothesis is stimulated by the fact that Cr as well as Mn_Z can take the part in a spin-flip transition due to a first-order magnetostructural transition from FM austenite to AFM martensite upon cooling. By using the *ab initio* methods combined with Monte Carlo (MC) technique, we have determined the initial magnetic reference states for austenite and martensite and simulated the temperature dependences of magnetization and magnetocaloric characteristics (ΔS_{mag} and ΔT_{ad}) of Co- and Cr-doping Ni-Mn-(In, Ga, Sn, and Al) alloys.

2 Microscopical Model

In order to simulate the temperature dependence of magnetic and magnetocaloric properties of polycrystalline Co- and Cr-doped Heusler alloys, we briefly review the Hamiltonian $\mathcal{H}$, which we will use in modelling functional properties[15, 14]. It consists of magnetic ($\mathcal{H}_{mag}$), elastic ($\mathcal{H}_{el}$), and magnetoelastic ($\mathcal{H}_{int}$) parts. For the magnetic term a Potts model with different q states for the magnetic atoms is used, for the elastic part the degenerated three-state Blume-Emery-Griffiths (BEG) model is used which allows to handle the structural transformation from cubic (austenitic) to the tetragonal (martensitic) phase. In detail, the Hamiltonian consists of:

$$\mathcal{H} = \mathcal{H}_{mag} + \mathcal{H}_{el} + \mathcal{H}_{int}, \tag{1}$$

where,

$$\mathcal{H}_{mag} = -\sum_{\langle ij \rangle} J_{ij}\,\delta_{S_i,S_j} + K_{ani}\sum_i \delta_{S_i,S_k}\mu_i^2 - g\mu_B H_{ext}\sum_i \delta_{S_i,S_g}\mu_i, \tag{2}$$

$$\begin{aligned}\mathcal{H}_{lat} &= -\sum_{\langle ij \rangle}\sigma_i\sigma_j\left\{J + g\mu_B H_{ext}\left(U_1\sum_i \delta_{S_i,S_g} + U_2 g\mu_B H_{ext}\right)\right\} \\ &\quad - K\sum_{\langle ij \rangle}\left(1-\sigma_i^2\right)\left(1-\sigma_j^2\right) - k_B T\ln(p)\sum_i\left(1-\sigma_i^2\right),\end{aligned} \tag{3}$$

$$\mathcal{H}_{int} = 2\sum_{\langle ij \rangle} U_{ij}\,\delta_{S_i,S_j}\mu_i\mu_j\left\{\left(\tfrac{1}{2}-\sigma_i^2\right)\left(\tfrac{1}{2}-\sigma_j^2\right) - \tfrac{1}{4}\right)\}. \tag{4}$$

Here, J_{ij} are the *ab initio* exchange coupling constants between magnetic moments μ_i at sites i and j of cubic and tetragonal Heusler lattices. S_i is the Potts spin at site i which can take on q integer values depending on the total spin moment S of an atom. The spin moment of Mn^{3+} ion is $S = 5/2$, hence, we associate the $2S + 1$ possible spin projections (-5/2, -3/2, -1/2, 1/2, 3/2, and 5/2) with the $q_{\mathrm{Mn}} = 1 \ldots 6$ states. Likewise, we assume $S = 1$, 3/2, and 4/2 for Ni^{2+}, Co^{2+}, and Cr^{2+} ions, respectively, with $q_{\mathrm{Ni}} = 1 \ldots 3$, $q_{\mathrm{Co}} = 1 \ldots 4$, and $q_{\mathrm{Cr}} = 1 \ldots 5$ states. K_{ani} is the magnetic anisotropic constant, H_{ext} is the external magnetic field, μ_B is Bohr's magneton, and g is the Landé factor. The Kronecker symbol, δ_{S_i,S_j}, restricts the spin-spin interactions to the interactions between the same S_i states for Mn, Co, Cr, and Ni. All spins in a magnetic domain have the same q state S_k, S_k may be chosen to be different from domain to domain. The coupling to the external magnetic field is specified by S_g where we align all spins by choosing $S_g = 1$ ($H_{ext} \geq 0$). For the magnetic interactions the bracket $\langle i, j \rangle$ denotes a sum over neighbors up to the sixth coordination shell. J and K are the structural coupling constants for the tetragonal and cubic states, which are responsible for the martensitic transition. The variable σ_i defines the deformation state at each lattice site where $\sigma_i = \pm 1$ and $\sigma_i = 0$ specify the tetragonal and cubic phases, respectively. p is the degeneracy factor of the cubic phase that characterizes the number of possible structural variants. U_{ij} are magnetoelastic interaction parameters while U_1 and U_2 are dimensionless magnetoelastic coupling constants [14]. The parameters U_1 and U_2 allow to realize the shift of structural transition temperature in an external magnetic field. The summation $\langle i, j \rangle$ in $\mathcal{H}_{el}$ is taken over nearest neighbor pairs.

Further information on the Hamiltonian can be found in Refs. [15, 14] and references therein. In summary, the Hamiltonian allows to account for a coupled magnetostructural phase transition which is needed for the description of the inverse MCE.

3 Computational Details

The equilibrium lattice parameters of austenite and martensite as well as the initial spin configurations of compounds were determined using the Quantum Espresso (QE)[1] codes in combination with the generalized gradient approximation for the exchange correlation functional in the formulation of Perdew, Burke and Ernzerhof (PBE)[11]. The energy calculations were performed for the 16-atom $L2_1$ supercell. In this way, the following compositions are used: $Ni_7Co_1Mn_5Cr_1In(Sn)_2$, $Ni_7Co_1Mn_4Cr_1Ga_3$, and $Ni_7Co_1Mn_6Al_2$ corresponding to $Ni_{43.75}Co_{6.25}Mn_{31.25}Cr_{6.25}In(Sn)_{12.5}$, $Ni_{43.75}Co_{6.25}Mn_{25}Cr_{6.25}Ga_{18.75}$ and $Ni_{43.75}Co_{6.25}Mn_{37.5}Al_{12.5}$, respectively. Calculations have been done for the FM state and three ferrimagnetic states(FIM-I, FIM-II, and FIM-III), shown in Figure 1.

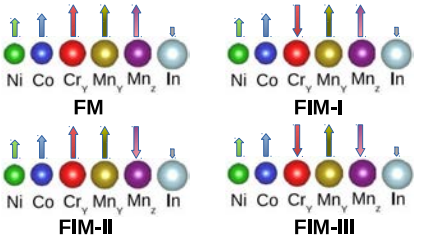

Figure 1: Different magnetic configurations taken into account in *ab initio* calculations. Here, arrows denote magnetic moments.

In order to calculate the magnetic exchange parameters J_{ij}, we used the SPR-KKR package[5] with the PBE potential and equilibrium lattice parameters obtained from the relaxation calculations. The chemical disorder in the off-stoichiometric Co- and Cr-doping Ni-Mn-(In, Ga, Sn, and Al) systems was treated with the coherent potential approximation (CPA). The exchange coupling constants were calculated using the full potential spin-polarized scalar-relativistic mode (FP SP-SREL).

Finally, using the Metropolis algorithm, we performed the MC simulations of the Potts-BEG Hamiltonian model for a lattice with a real unit cell consisting of 3925 atoms. For off-stoichiometric $Ni_{2-y}Co_yMn_{1+x-z}Cr_zZ_{1-x}$ alloys, we assume that fractions of Mn_Z (x), Cr (z), and Co (y) are randomly distributed on the Z, Mn_Y and Ni sublattices, respectively, according to the alloy composition. As time unit, we used one MC step consisting of N attempts to change the variables $q_{\rm Ni}$, $q_{\rm Co}$, $q_{\rm Cr}$, $q_{\rm Mn_{Y(Z)}}$ and σ_i. For each temperature the properties of the system (internal energy and order parameters) were analyzed allowing $5 \cdot 10^5$ MC steps and 10^4 thermalization steps. In order to create the multi-domain (cluster) state, we divided the simulation cell into 16 equal clusters with initial random q-Potts variables [15, 14].

With respect to the J_{ij} parameters, which are shown in Figure 2, we have truncated the magnetic interactions at a distance of $1.85a_0$. Since, the magnetic anisotropy energy (MAE) of martensite (M) is much larger compared with the MAE of austenite (A), we used a value of K_{ani}(M). With respect to the elastic part of the Hamiltonian, we limited for simplicity the structural interactions between all atoms to the first coordination shell. As a result, parameters J and K and dimensionless magnetoelastic interaction constants, U_1 and U_2, have been used as fit parameters in order to reproduce the experimental martensitic transformation temperature, T_m, and dT_m/dH_{ext}. This is a rather crude approximation in view of the dipole-like long-range nature of elastic interactions, but, it allows reasonable simulation times. In principle, the structural coupling parameters can be estimated from first-principles.

The model parameters are listed in Table 1.

Composition	J	K	U_{ij}	U_1	U_2	K^A_{ani}	K^M_{ani}
$Ni_{45}Co_5Mn_{32}Cr_5In_{13}$	6.6	1.57	0.5	-1.2	-0.3	0.1	0.0001
$Ni_{41}Co_9Mn_{25}Cr_5Ga_{20}$	6.35	0.5	0.2	-0.5	-0.2	0.1	0.0001
$Ni_{40}Co_{10}Mn_{34}In_{16}$	7.6	1.5	0.5	-1.2	-0.9	0.05	0.0005

Table 1: The model parameters which have been used in the MC simulations of Co- and Cr-doped Ni-Mn-(In, Ga, Al) alloys. Here, the parameters J, K, U_{ij}, and K_{ani} are given in meV, U_1 and U_2 are dimensionless parameters and mark the strength of magnetoelastic interaction.

4 Results of *Ab initio* and Monte Carlo Calculations

The exchange coupling parameters for stable spin states and structures of Co- and Cr-doped Ni-Mn-(In, Sn, Ga, and Al) compositions are shown in Figure 2. Note, we have found from our supercell calculations that the FM spin alignment is the stable state of all austenite compositions while the FIM-II and FIM-III spin configurations are energetically favorable in martensite of Ni-Co-Mn-(Cr)-(Ga, Al) and Ni-Co-Mn-Cr-(In, Sn) compounds, respectively. In all cases the inter-sublattice interactions ($Mn_{Y(Z)}$-Co, $Mn_{Y(Z)}$-Ni, $Mn_{Y(Z)}$-$Mn_{Y(Z)}$, $Mn_{Y(Z)}$-Cr, and Cr-Co) provide the largest contribution to the exchange compared to the intra-sublattice interactions ($Mn_{Y(Z)}$-$Mn_{Y(Z)}$, Co-Co, Ni-Ni, and Cr-Cr). Moreover, $Mn_{Y(Z)}$-Co and $Mn_{Y(Z)}$-Ni interactions are largest in austenite for instead of all alloys. Hence the FM order (and high T_C) of

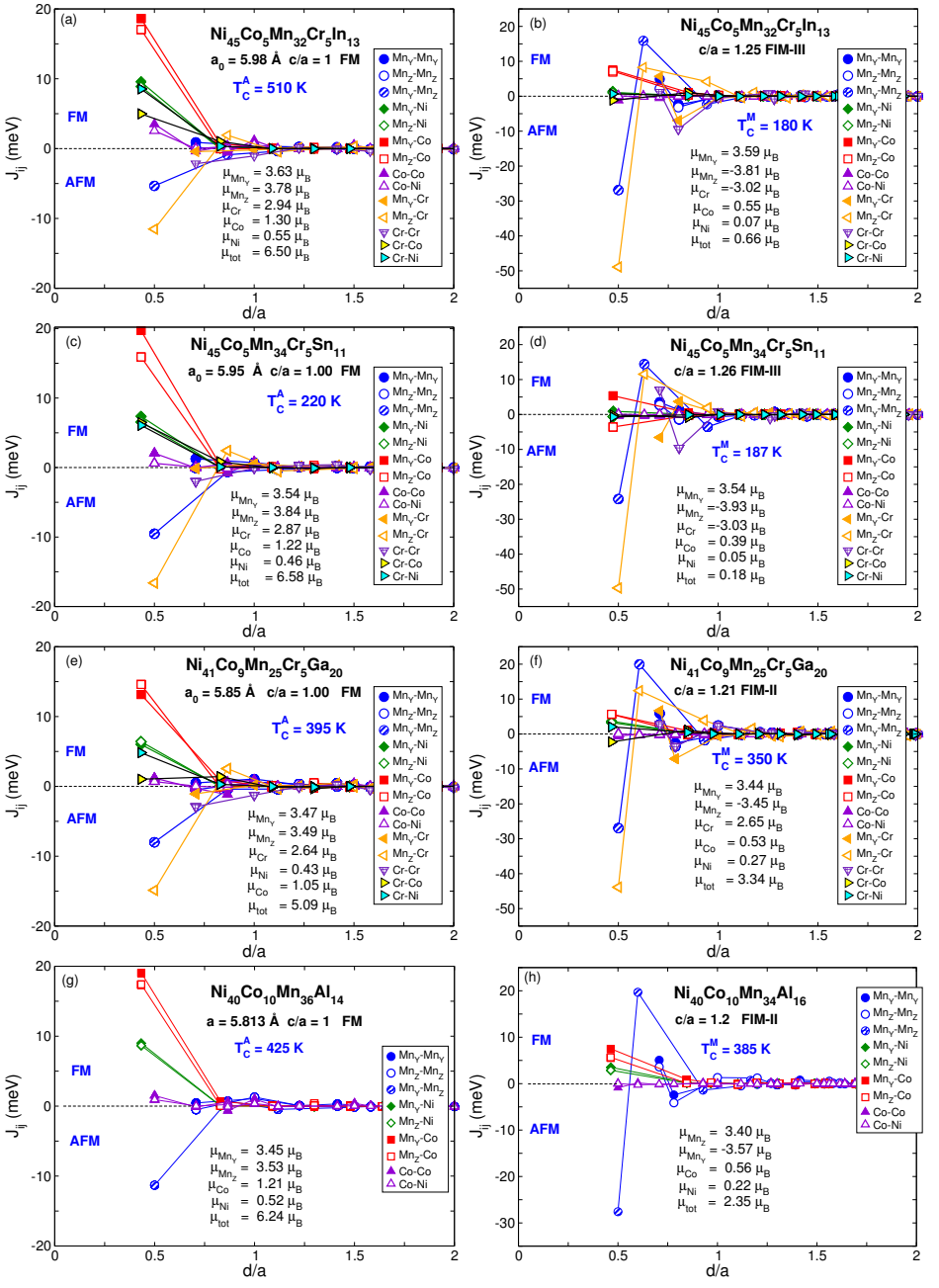

Figure 2: (a) Calculated magnetic exchange couplings of Co- and Cr-doped Ni-Mn-(In, Sn, Ga, and Al) alloys for the FM cubic phase and FIM-II and FIM-III tetragonal phases. Here, results for (a, b) $Ni_{45}Co_5Mn_{32}Cr_5In_{13}$, (c, d) $Ni_{45}Co_5Mn_{34}Cr_5Sn_{11}$, (e, f) $Ni_{41}Co_9Mn_{25}Cr_5Ga_{20}$, and (g, h) $Ni_{40}Co_{10}Mn_{34}Al_{16}$ alloys. T_C^A and T_C^M mark the Curie temperatures of austenite and martensite obtained from MC simulations.

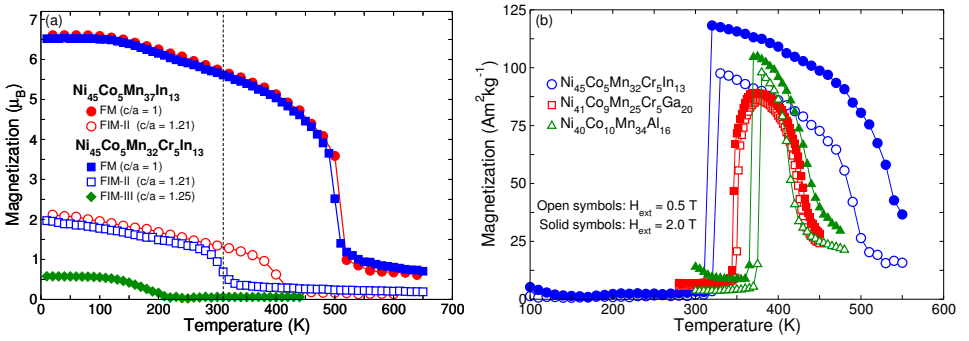

Figure 3: (a) Thermomagnetization curves of Co- and Cr-doped Ni-Mn-In alloys calculated for FM austenite and martensite with FIM-II and FIM-III orders in zero magnetic field. The T_m temperature is marked by the dashed line. (b) Magnetization curves of Co- and Cr-doped Ni-Mn-(In, Ga, Al) as functions of temperature in fields of 0.5 and 2 T.

austenite is stabilized by the $Mn_{Y(Z)}$-Co and $Mn_{Y(Z)}$-Ni interactions. We also can observe that the Mn_Y-Mn_Z exchange in the first coordination shell becomes approximately four times larger in martensite compared to austenite. The origin of this large AFM Mn_Y-Mn_Z exchange is related to the shorter distance of Mn_Y and Mn_Z compared to $Mn_{Y(Z)}$-$Mn_{Y(Z)}$ positions. In the case of martensite it is seen that the nearest Mn_Y-Mn_Z exchange for all compounds has a large AFM value ($\approx$ -25 meV), then changes sign and reaches a large FM value ($\approx$ 15 meV) in the next coordination shell. With respect to the magnetic exchange involving Cr, it is obvious that the strongest AFM interaction ($J_{ij} \approx -50$ meV) between nearest $Mn_{Y(Z)}$-Cr atoms is observed for the martensitic phase while Cr-Co(Ni), and Co-Co(Ni) coupling constants are close to zero.

By using the Potts-BEG Hamiltonian in combination with *ab initio* input data, we simulated temperature dependences of magnetic and magnetocaloric properties. We first have modeled the magnetization of $Ni_{45}Co_5Mn_{32}Cr_5In_{13}$ by employing the J_{ij} exchange parameters of FM austenite and FIM-II(FIM-III) martensite and compared these results with the magnetization curves obtained for $Ni_{45}Co_5Mn_{37}In_{13}$. This was done by using only the magnetic part of the total Hamiltonian ($\mathcal{H}_{lat} = 0, \mathcal{H}_{int} = 0, H_{ext} = 0, K_{ani} = 0$), without any influence from the structural subsystem. The total magnetization obtained in this way for austenitic and martensitic structures of Co- and Cr-doped Ni-Mn-In alloy is displayed in Figure 3(a). The magnetization behavior for FM austenite of both $Ni_{45}Co_5Mn_{37}In_{13}$ and $Ni_{45}Co_5Mn_{32}Cr_5In_{13}$ alloys is approximately similar because of the very similar behavior of J_{ij}. With respect to magnetizations of martensitic phases, we observe that in case of initial FIM-III spin state of martensite, magnetization and, correspondingly, the T_C of martensite are found to be drastically reduced as compared to the FIM-II configuration. Assuming that the transformation from martensite to austenite will occur around 310 K, see the dashed line in Figure 3(a), we find a wide paramagnetic gap below T_m. Note that the choice of T_m is reasonable because T_m of $Ni_{45}Co_5Mn_{37}In_{13}$ is equal to $\approx$ 310 K [10]. In this work, we propose that the T_m is not strongly shifted with addition of 5 at.% Cr. We understand that this is a crude approximation, however, it helps to perform the MC simulations of magnetocaloric properties of Co- and Cr-doped Ni-Mn-(In, Ga, Al) alloys with the help of our Hamiltonian. In Figure 3(b) we show the isofield magnetization curves of Co- and Cr-doped Ni-Mn-(In, Ga, Al) in magnetic fields of 5 mT and 2 T. Note that the thermomagnetization curves for Ni-Co-Cr-Mn-Sn system is not presented here because of small values of T_C^A and T_C^M. Besides, these values are closed to each other. Here, we

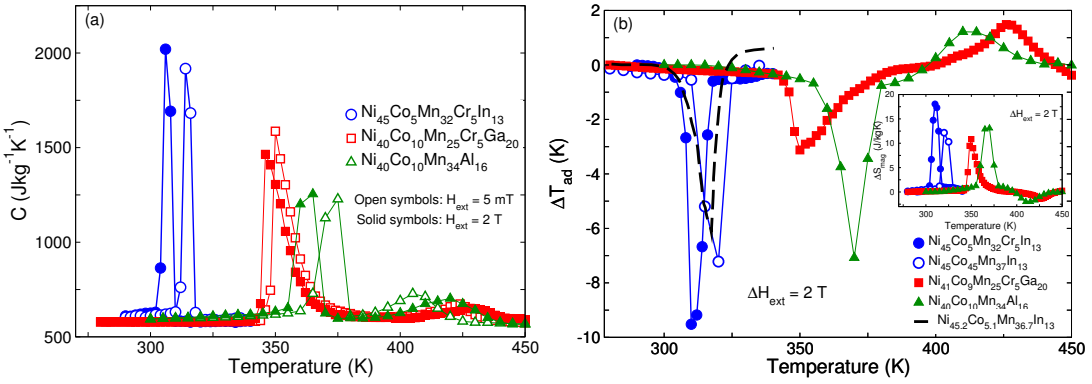

Figure 4: The temperature dependence of (a) total specific heat and (d) adiabatic temperature change of Co- and Cr-doped Ni-Mn-(In, Ga, Al) alloys in a magnetic field change of 2 T. The inset shows the isothermal magnetic entropy changes of Co- and Cr-doped Ni-Mn-(In, Ga, Al) alloys at $\Delta H_{ext} = 2$ T obtained by integrating corresponding specific heat curves. Experimental MCE for $Ni_{45.2}Co_{5.1}Mn_{36.7}In_{13}$ is shown by dashed lines which were measured in $\Delta H_{ext} \approx 1.9$ T by Liu *et al.*[10].

observe two phase transitions upon cooling, which are corresponded to the para-ferromagnetic transition in the austenite and the magnetostructural transition from FM austenite to the low-magnetic or non-magnetic martensite. In addition, large changes in the magnetization around T_m as well as the negative shift of T_m in the external magnetic field can be seen in figure 3(b).

The total specific heats of Co- and Cr-doped Ni-Mn-(In, Ga, Al) alloys in magnetic fields of 0 and 2 T are shown in Figure 4(a). We can observe that the peaks of a specific heat curves are shifted towards lower temperature when the magnetic field is applied. Such behavior is due to the metamagnetic phase transition in combination with austenite-martensite structural transformation.The theoretical magnetocaloric characteristics, $\Delta S_{mag}(T)$ and $\Delta T_{ad}(T)$, for Co- and Cr-doped Ni-Mn-(In, Ga, Al) in combination with experimental behavior of ΔT_{ad} for $Ni_{45}Co_5Mn_{32}Cr_5In_{13}$ are presented in Figure 4(b). It is seen that that the addition of Co and Cr results in large values of the inverse MCE. Moreover, the largest MCE is found to be of ($\Delta T_{ad} \approx$-9 K) in the $Ni_{45}Co_5Mn_{32}Cr_5In_{13}$ alloy assuming the martensite with FIM-III order.

5 Conclusions

In summary, we have combined *ab initio* with Monte Carlo approaches to investigate the influence of Cr addition on the magnetic and magnetocaloric properties of of Co- and Cr-doped Ni-Mn-(In, Sn, Ga, Al) alloys. The density functional theory simulations have shown that the addition of Cr in Ni-Co-Mn-(In, Sn) results in an appearance of the magnetostructural transition from FM austenite to FIM-III martensite, while in the case of Ni-Co-Mn-Cr-Ga system, the martensitic transformation from FM austenite to FIM-II martensite is found. In regard to exchange coupling constants in martensite, the addition of Cr results in the enhancement of AFM exchange interactions between $Mn_{Y(Z)}$-Cr and Mn_Y-Mn_Z atoms as well as Cr-Cr sites. As a consequence, the large changes in magnetization for Co- and Cr-doped Ni-Mn-(In, Ga, Al) alloys are observed. This is due to the fact that the Cr and Mn_Y magnetic moments change their orientation between martensite and austenite. In contrast, for Ni-Co-Mn-Sn system the addi-

tion of Cr does not sufficiently increase the change in magnetization because of smaller Curie temperatures of austenite and martensite and larger AFM exchange interactions in austenite and martensite. As a result, the influence of Cr and Co on the MCE in Ni-Mn-(In, Ga, Al) leads to an increase of the inverse MCE as compared to Ni-Co-Mn-Sn. It is worth noting that the synthesizing of Heusler alloys with a high total magnetic moment in austenite and a low total magnetic moment in martensite is the key to resolve the problem of MCE optimization.

6 Acknowledgments

This work is supported by RFBR Grant No. 14-02-01085, RSF No. 14-12-00570\14 (Section 2 and 3), Ministry of Education and Science of RF No 3.2021.2014/K (Section 4) PE acknowledges DFG (SPP 1599) for financial support.

References

[1] Quantum ESPRESSO package Version 5.02. `http://www.pwscf.org`.

[2] V.D. Buchelnikov and V.V. Sokolovskiy. Magnetocaloric effect in NiMnX (X = Ga, In, Sn, Sb) Heusler alloys. *Phys. Metal. Metallogrh.*, 112:633–29, 2011.

[3] Ö. Çakir and M. Acet. Reversibility in the inverse magnetocaloric effect in Mn_3GaC studied by direct adiabatic temperature-change measurements. *Appl. Phys. Lett.*, 100:202404–3, 2012.

[4] D.Y. Cong, S. Roth, and L. Schultz. Magnetic properties and structural transformations in Ni-Co-Mn-Sn multifunctional alloys. *Acta Mater.*, 60:5335–5351, 2012.

[5] H. Ebert. SPR-KKR package Version 6.3. `http://ebert.cup.uni-muenchen.de`.

[6] S. Fabbrici, G. Porcari, F. Cugini, M. Solzi, J. Kamarad, Z. Arnold, R. Cabassi, and F. Albertini. Co and In Doped Ni-Mn-Ga Magnetic Shape Memory Alloys: A Thorough Structural, Magnetic and Magnetocaloric Study. *Entropy*, 16:2204–2222, 2014.

[7] V. Franco, J.S. Blázquez, B. Ingalge, and A. Conde. The magnetocaloric effect and magnetic refrigeration near room temperature: materials and models. *Annu. Rev. Mater. Res.*, 42:305–342, 2012.

[8] K.A. Gschneidner Jr. and V.K. Pecharsky. Thirty years of near room temperature magnetic cooling: Where we are today and future prospects. *Int. J. Refrig.*, 31:945–961, 2005.

[9] K.A. Gschneidner Jr., V.K. Pecharsky, and A.O. Tsokol. Recent developments in magnetocaloric materials. *Rep. Prog. Phys.*, 68:1479–1539, 2005.

[10] J. Liu, T. Gottschall, K.P. Skokov, J.D. Moore, and O. Gutfleisch. Giant magnetocaloric effect driven by structural transitions. *Nature Mater.*, 11:620–626, 2012.

[11] J.P. Perdew, K. Burke, and M. Enzerhof. Generalized Gradient Approximation Made Simple. *Phys. Rev. Lett.*, 77:3865–3868, 1996.

[12] A. Planes, Ll. Ma nosa, and M. Acet. Magnetocaloric effect and its relation to shape-memory properties in ferromagnetic heusler alloys. *J. Phys.: Condens. Matter.*, 21:233201–29, 2009.

[13] K.G. Sandeman. Magnetocaloric materials: The search for new systems. *Scripta Mater.*, 67:566–571, 2012.

[14] V.V. Sokolovskiy, A. Grünebohm, V.D. Buchelnikov, and P. Entel. *Ab Initio* and Monte Carlo Approaches For the Magnetocaloric Effect in Co- and In-Doped Ni-Mn-Ga Heusler Alloys. *Entropy*, 16:4992–5019, 2014.

[15] V.V. Sokolovskiy, V.D. Buchelnikov O.O. Pavlukhina, and P. Entel. Monte Carlo and first-principles approaches for single crystal and polycrystalline Ni_2MnGa Heusler alloys. *J. Phys. D: Appl. Phys.*, 47:425002–13, 2014.